GEOPHYSICAL RESEARCH LETTERS, VOL. 26, NO. 8, PAGES 1077-1080, APRIL 15, 1999

A Shallow-Dipping Dike fed the 1995 Flank Eruption at Fernandina Volcano, Galápagos, Observed by Satellite Radar Interferometry

Sigurjón Jónsson, Howard Zebker, Peter Cervelli, Paul Segall

Geophysics Department, Stanford University, California

Harold Garbeil, Peter Mouginis-Mark, Scott Rowland

Hawaii Institute of Geophysics and Planetology, University of Hawaii, Honolulu

Abstract. Satellite radar interferometry data reveal strong localized uplift in a semi- circular pattern on the southwest flank of Fernandina volcano, Galápagos, where an eruption took place in January to April, 1995. The observations show a maximum decrease in radar range of 0.75 m, and they are consistent with a model of a shallow-dipping dike intrusion feeding this fissure eruption. We solve for the best-fit single rectangular dislocation dike source using non-linear inversion techniques where simulated annealing searching algorithm is used to avoid local minima. The best-fit dike is 3.8 km long, 2.3 km high, 0.86 m thick and with a 34° dip. The total dike volume (7.5×10^{-3} km^3) is ∼40% of the volume of extrusive materials estimated to have been produced during the eruption. The data do not permit a sub-vertical dike, implying that the least principal stress direction is not horizontal as is usually assumed.

Introduction

The Galápagos archipelago is located on the Nazca plate about 1000 km west of Ecuador, just south of the east-west trending Galápagos spreading center (Fig. 1a). The islands are a cluster of about 20 basaltic volcanoes that typically have large summit calderas. Unlike Hawaiian basaltic volcanoes, they do not have well-developed rift zones, but instead have a pattern of arcuate vents near the caldera rim and radial vents further away on the flanks [*Chadwick and Howard,* 1991].

Fernandina Island is about 30 km in diameter and consists of a single volcano with a maximum elevation of 1470 m with a nearly 1000 m deep central caldera [*Rowland,* 1996] (Fig. 1b). Fernandina is among the most active volcanoes in the world; it erupted at least 13 times during 1950-1998 [*Rowland and Munro,* 1992]. The eruption of 1968 was followed by the largest historical caldera collapse on any basaltic volcano, with a maximum subsidence of about 300 m [*Simkin and Howard,* 1970]. The most recent activity at Fernandina includes intracaldera eruptions in 1988 and 1991, and a radial fissure eruption on the SW flank in 1995 [*Chadwick et al.,* 1991; *Rowland and Munro,* 1992; *Global Volcanism Network,* 1995; *Wooster and Rothery,* 1997].

Paper number 1999GL900108.
0094-8276/99/1999GL900108$05.00

The 1995 eruption began on around January 25 and lasted for about 10 weeks [*Global Volcanism Network,* 1995]. The uppermost vents at elevations of 600-1100 m produced a negligible amount of lava [*Rowland,* 1996]. The main vent was located at 250 m elevation and produced about 0.02 km^3 lava, assuming a 3 m average thickness [*Wooster and Roth-*

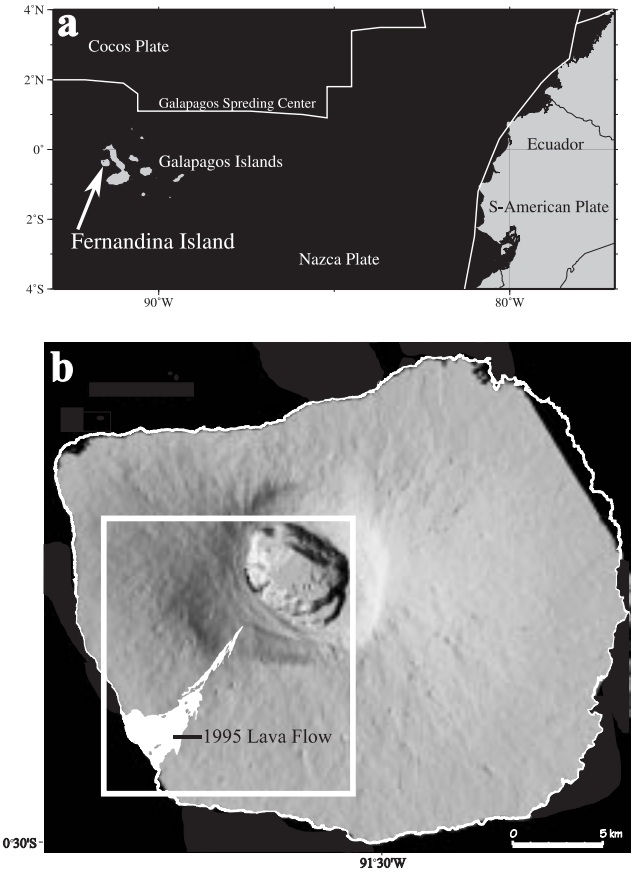

Figure 1. a) Galapagos Islands are located about 1000 km west of Ecuador on the Nazca plate, just south of the Galapagos spreading center. Fernandina Island is the westernmost island in the archipelago. White lines mark plate boundaries. b) A shaded relief map of Fernandina Island. The area covered by the 1995 lava flows is showed on the SW flank as mapped from a SPOT image [*Rowland,* 1996]. The box marks the area covered in Fig. 2.

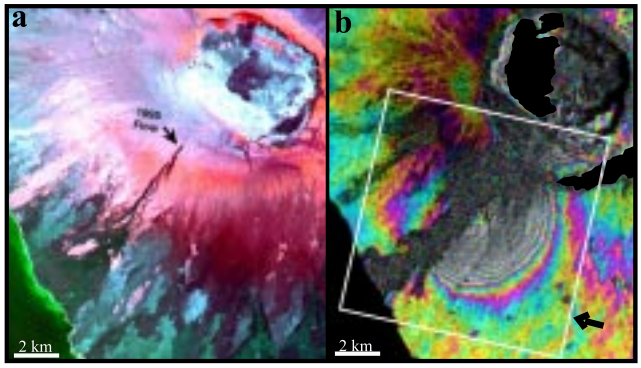

Figure 2. a) A SPOT image of the SW flank of Fernandina Volcano from July 6, 1995. Red colors denote vegetated areas. The upper part of the 1995 lava flow can clearly be seen where it covered an area of relatively dense vegetation, but it is less clear near the coast. © SPOT image 1995. b) The 1992-1997 interferogram of the SW flank of Fernandina. The arrow indicates the look direction of the satellite down from the ESE. The strong semi-circular pattern has a maximum decrease in radar range of about 27 fringes, or 0.75 m, representing mostly uplift above the intrusion. The box marks the area covered in Fig. 3.

ery, 1997]. The lava covered a subaerial area of 8.2 km^2 extending 9 km from the uppermost vent to the ocean [*Rowland,* 1996].

Here we examine the 1995 eruption using Synthetic Aperture Radar (SAR) interferometry satellite data. SAR has proven to be an important tool for investigating crustal deformation and dynamics of active volcanoes, e.g. at Etna volcano in Italy and Krafla volcano, Iceland [*Massonnet et al.,* 1995; *Lanari et al.,* 1998; *Sigmundsson et al.,* 1997].

Data Analysis and Results

We present data from the European satellites ERS-1 and 2 acquired over Fernandina in 1992 and 1997. Two interferograms were formed, an interferogram spanning the five years (Sept. 12, 1992 - Sept. 30, 1997) and an interferogram that spans only one day (Sept. 29-30, 1997). Both interferograms include phase information about the island's topography but the five-year interferogram additionally has information about the deformation that occurred during this time span [*Zebker et al.,* 1994].

We isolated the deformation signature by two different methods, revealing the same results. First, we removed the topographic effect using the three-pass method [*Zebker et al.,* 1994], using the one-day interferogram as a reference. We also removed the topography using the two-pass approach [*Massonnet et al.,* 1993], producing a simulated interferogram from a pre- existing Digital Elevation Model (DEM) and subtracting it from the five-year interferogram. In the latter, we used a DEM generated during the 1993 airborne Topographic Synthetic Aperture Radar (TOPSAR) mission to the Galapagos Islands [*Rowland,* 1996; *Zebker et al.,* 1992]. This second approach gives a more complete differential interferogram, because in certain areas near the caldera, the topographic information in the one-day interferogram is lost due to decorrelation. We also avoid estimating a second set of baselines and are free of possible atmospheric disturbances that may be included in the one-day interferogram. Both resulting differential interferograms contain phase signatures mainly from deformation that occurred during the five years from 1992 to 1997.

We unwrapped the phase of the two-pass differential interferogram (Fig. 2b) using the residue-cut algorithm of *Goldstein et al.* [1988] to obtain absolute values of the range changes for each pixel rather than ambiguous phase values ranging from 0 to 2π. The whole interferogram of the island unwrapped readily, except where surface scattering changed over the five years, e.g. on areas of relatively dense vegetation near the caldera, and on the area covered by the 1995 lava flow [*Zebker et al.,* 1996] (Fig. 2a-b and 3a).

The five-year differential interferograms reveal a strong semi-circular signal of range decrease on the SW flank of the volcano. The signal of about 27 28-mm-fringes represents 0.75 m of decrease in range, i.e. the ground moving towards the radar (Fig. 2b and 3a). Since the ERS SARs have an incidence angle of 23° from vertical this is presumably mainly uplift. The deformation pattern is not purely semi-circular in nature. The amplitude of the deformation pattern decreases from its maximum towards the caldera with a minimum at 2 km from the caldera rim, where it increases again (Fig. 2b). This increase likely results from a second subsurface feature, but the incomplete nature of the signature due to decorrelation precludes simple analy-

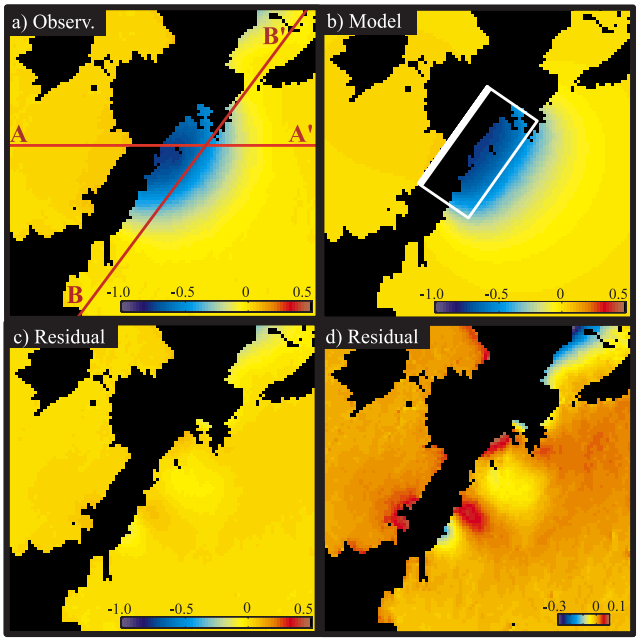

Figure 3. a) The unwrapped interferogram gives absolute values of the range change. The scale shows range change in meters. Marked in black is the area that could not be unwrapped because of decorrelation, partly due to the 1995 lava flow. Profiles A-A' and B-B' are shown in Fig. 4. b) The best-fit model of a shallow-dipping dike presented in radar coordinates. The white rectangle marks the projection of the best-fit dike onto the surface, and the thick sideline indicates where it hits the surface. d) The residual between the observations (Fig. 3a) and the model (Fig. 3b). d) Same as Fig. 3c, except another color scale.

Table 1. The parameters for the best-fit dike. Uncertainties show 95% confidence.

Length (km)	Height (km)	Depth (km)	Dip (°)	Strike (N°E)	Opening (m)	Volume (km^3)	Lat. (°S)	Long. (°W)
$3.8^{+0.1}_{-0.1}$	$2.3^{+0.1}_{-0.8}$	$0.0^{+0.0}_{-0.5}$	34^{+15}_{-3}	47^{+8}_{-3}	$0.86^{+0.21}_{-0.01}$	$\left[7.5^{+0.4}_{-1.4}\right] \times 10^{-3}$	$0.414^{+0.0km}_{-0.4km}$	$91.585^{+0.0km}_{-0.5km}$

sis, hence an interpretation of the larger deformation pattern only is given below. Another, much smaller, semi-circular pattern is observed on the western side of the 1995 lava flow. This signal has an opposite sign, representing an increase in range of about two fringes, or 58 mm (Fig. 2b).

Modelling

We use a single rectangular dislocation surface in an elastic half- space [*Okada,* 1985] to simulate ground deformation due to a dike intrusion. Ten parameters define the dislocation: length, height, strike, dip, and location (three parameters) and the three parameters of displacement across the dislocation: dip-slip, strike-slip, and opening. In the inversion we constrain the dip-slip and the strike-slip to be zero because no radial faulting has been observed on Fernandina; other parameters are freely determined. We use a simulated annealing algorithm to avoid local minima in this non-linear problem [*Cervelli et al.,* 1997]. The covariance matrix is assumed to be diagonal, i.e. errors of the range change observations are taken to be independent of one another. Because the correlations vary from one interferogram to another, and because wavelengths and amplitudes of atmospheric disturbances vary from place to place and from one day to another [*Zebker et al.,* 1997], this assumption could slightly distort our estimate of the source geometry.

The resulting best-fit model is a gently dipping dike, about 3.8 km long, 2.3 km high, 0.86 m thick, striking N47°E, and dipping 34° from horizontal to the SE (Table 1). The inversion places the upper edge of the dike at the surface, coincident with where the eruption took place. Fig. 3b shows the deformation in radar coordinates as predicted by the model; it matches the observations with less than 0.05 m residual over most of the signal (Fig. 3c-d). Profiles showing range changes across the observed area are compared to the modeling results in Fig. 4. Sensitivity analysis of the inversion procedure using bootstrap techniques [*Efron and Tibshirani,* 1993] shows that the dike length, depth, and opening are relatively well resolved, but the dike dip and the dike height are less well constrained (Table 1). The volume of the best-fit dike is found to be 7.5×10^{-3} km^3, or around 40% of the estimated lava volume.

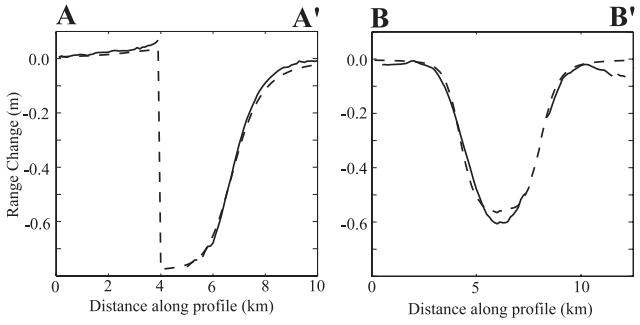

Figure 4. Comparison of observed (solid lines) and modeled (ticked lines) range changes along profiles A-A' and B-B' in Fig. 3a and 3b (profiles only showed in Fig. 3a).

Discussion and Conclusions

Our estimation of the dike geometry gives new unexpected information about the stress field at Fernandina volcano. Geological investigations show that vents and presumably underlying dikes on the caldera rim have an arcuate, caldera-parallel orientation, but vents further away from the rim have radial orientations [*Chadwick and Howard,* 1991; *Rowland,* 1996]. Because the minimum compressional stress, σ_3, is generally perpendicular to dikes, it has a radial orientation at the caldera-rim, and is circumferential further down the volcano. Hence, the two categories of vents at Fernandina volcano indicate a change in the stress field from the caldera rim down to the flanks [*Chadwick and Dieterich,* 1995]. A few circumferential dikes on Fernandina are exposed in the caldera wall. There they are observed to be vertical or nearly vertical, and they are about 1 m thick [*Chadwick and Howard,* 1991]. Even though the orientation of the minimum compressional stress axis changes from the near-caldera region out to the flanks, it has been assumed that the axis would still be horizontal [*Chadwick and Dieterich,* 1995]. In other words, the radial dikes have been considered vertical as well. Our best-fit model of the 1995 radial dike intrusion is far from being vertical, it has a tilt of about 34° from horizontal. This indicates not only a rotation of the minimum compressional stress axis in the horizontal plane about the vertical axis, from the caldera-rim down to the flanks, but also a rotation about a horizontal axis, at least at shallow depths.

No conventional geodetic network exists on Fernandina, so if not for SAR observations, we would know little about this event, except that a radial dike intruded and reached the surface. While our spatial coverage of the Fernandina event is very good, consisting of thousands of observations on an area as little as 4×6 km, our temporal resolution is quite limited since we could only difference two scenes acquired in 1992 and 1997. However, we have been able to constrain parameters and dimensions of the dike intrusion relatively well.

In summary, ERS radar interferograms of Fernandina volcano permit detailed spatial observation and analysis of crustal deformation, such as the 1995 dike emplacement. We find that a non-linear inversion of the data, using a single rectangular dislocation source, results in a dike that is 3.8 km long, 2.3 km high, 0.86 m thick, and dipping 34° to the SE. In addition, the dip of the best-fit dike indicates that the orientation of σ_3 may not only rotate about the vertical axis from the caldera-rim out to the flanks, but also about a horizontal axis, at least at shallow depths.

Acknowledgments. We thank Falk Amelung (Stanford University) for the help with the data processing. Comments made by Mark Simons and an anonymous reviewer improved the manuscript.

References

Cervelli, P., P. Segall, and Y. Aoki, Simulated annealing for inverting surface displacements for fault slip and geometry, with an application to the 1994 earthquake swarm off the Izu peninsula of Japan (abstract), *EOS Trans., AGU 78(46)*, Fall Meet. Suppl., p159, 1997.

Chadwick Jr, W. W., and K. A. Howard, The pattern of circumferential and radial eruptive fissures on the volcanoes of Fernandina and Isabela islands, Galapagos, *Bull. Volcanol., 53,* 259-275, 1991.

Chadwick Jr, W. W., T. De Roy, and A. Carrasco, The September 1988 intracaldera avalanche and eruption at Fernandina volcano, Galapagos Islands, *Bull. Volcanol., 53,* 276-286, 1991.

Chadwick Jr, W. W., and J. H. Dieterich, Mechanical modeling of circumferential and radial dike intrusion on Galapagos volcanoes, *J. Volcanol. Geotherm. Res., 66*, 37-52, 1995.

Efron, B., and R. J. Tibshirani, *An introduction to the bootstrap*, Monogr. on Stat. and Appl. Probab. 57, 436 pp., Chapman & Hill, New York, 1993.

Global Volcanism Network, Smithsonian Inst. Bull., *20(1-3, 5, 8),* 1995.

Goldstein R. M., H. A. Zebker, and C. Werner, Satellite radar interferometry: Two-dimensional phase unwrapping, *Radio Sci., 23,* 713-720, 1988.

Lanari, R., P. Lundgren, and E. Sansosti, Dynamic deformation of Etna volcano observed by satellite radar interferometry, *Geophys. Res. Lett., 25,* 1541-1544, 1998.

Massonnet, D., M. Rossi, C. Carmona, F. Adragna, G. Peltzer, K. Feigl, and T. Rabaute, The displacement field of the Landers earthquake mapped by radar interferometry, *Nature, 364,* 138-142, 1993.

Massonnet, D., P. Briole, and A. Arnaud, Deflation of Mount Etna monitored by spaceborne radar interferometry, *Nature, 375,* 567-570, 1995.

Okada, Y., Surface deformation due to shear and tensile faults in a half-space, *Bull. Seism. Soc. Am., 75,* 1135-1154, 1985.

Rowland, S. K., and D. C. Munro, The caldera of volcan Fernandina: a remote sensing study of its structure and recent activity, *Bull. Volcanol., 55,* 97-109, 1992.

Rowland, S. K., Slopes, lava flow volumes, and vent distributions on volcán Fernandina, Galápagos islands, *J. Geophys. Res., 101*, 27,657-27,672, 1996.

Sigmundsson, F., H. Vadon, and D. Massonnet, Readjustment of the Krafla spreading segment to crustal rifting measured by satellite radar interferometry, *Geophys. Res. Lett., 24*, 1843-1846, 1997.

Simkin, T., and K. A. Howard, Caldera collapse in the Galápagos islands, 1968, *Science, 169,* 429-437, 1970.

Wooster, M. J., and D. A. Rothery, Time-series analysis of effusive volcanic activity using the ERS along track scanning radiometer: The 1995 eruption of Fernandina volcano, Galápagos islands *Remote Sens. Environ., 62,* 109- 117, 1997.

Zebker, H. A., S. N. Madsen, J. Martin, K. B. Wheeler, T. Miller, Y. Lou, G. Alberti, S. Vetrella, and A. Cucci, The TOPSAR interferometric radar topographic mapping instrument, *IEEE Trans. Geosci. Remote Sens., 30,* 933-940, 1992.

Zebker, H. A., P. A. Rosen, R. M. Goldstein, A. Gabriel, and C. L. Werner, On the derivation of coseismic displacement fields using differential radar interferometry: The Landers earthquake, *J. Geophys. Res., 99,* 19,617-19,634, 1994.

Zebker, H. A., P. Rosen, S. Hensley, P. Mouginis-Mark, Analysis of active lava flows on Kilauea volcano, Hawaii, using SIR-C radar correlation measurements, *Geology, 24,* 495-498, 1996.

Zebker, H. A., P. A. Rosen, and S. Hensley, Atmospheric effects in interferometric synthetic aperture radar surface deformation and topographic maps, *J. Geophys. Res., 102,* 7547-7563, 1997.

P. Cervelli, S. Jónsson, P. Segall, H. Zebker, Geophysics Department, Stanford University, Stanford, CA 94305-2215, USA (e-mail: jonsson@pangea.stanford.edu)

H. Garbeil, P. Mouginis-Mark, S. Rowland, Hawaii Institute of Geophysics and Planetology, University of Hawaii, 2525 Correa Rd., Honolulu, HI 96822, USA

(Received November 13, 1998; revised February 9, 1999; accepted February 11, 1999.)